Low-Valent Iron Porphyrins. NMR Evidence for π-Anion-Radical Character in Two-Electron-Reduced Iron(III) Meso- or β-Pyrrole-Substituted Porphyrins

Kazuya Yamaguchi and Isao Morishima*

Division of Molecular Engineering, Graduate School of Engineering, Kyoto University, Kyoto 606, Japan

Received November 19, 1991

Absorption, electron spin resonance (ESR), solution magnetic susceptibility, and proton and deuterium NMR data are reported for the two-electron-reduction products $[FePor]^-$ (Por = porphyrin) of a series of Fe(III) porphyrins substituted at the meso or β-pyrrole position(s) by electron-withdrawing groups. Upon reduction, the meso-deuterium resonances of *meso*-nitro-$[FeOEP]^-$ (OEP = octaethylporphyrin) exhibited unusually large upfield hyperfine shifts (230 ppm), the α-methylene proton resonances were shifted far downfield, and the reduced product afforded a magnetic susceptibility of $\mu_{eff} = 5.7\ \mu_B$. NMR hyperfine shifts and other physical data for *meso*-nitro-$[FeOEP]^-$ are in accordance with the formulation of a ferrous high-spin ($S = 2$) porphyrin π-anion radical ($S = {}^1/_2$). *meso*-Chloro-, *meso*-formyl-, and *meso*-cyano-$[FeOEP]^-$ and *β-pyrrole*-tetrabromo-$[FeTPP]^-$ were identified as Fe(I) porphyrins with low-spin states, as observed for unsubstituted $[Fe^IOEP]^-$ and $[Fe^ITPP]^-$ complexes. It was also suggested that *β-pyrrole*-tetracyano-$[FeTPP]^-$ could be formulated as the resonance hybrid of two extreme structures: an Fe(I) porphyrin and an Fe(II) porphyrin π-anion radical.

Introduction

Two-electron-reduction products ($[FePor]^-$) of iron(III) porphyrins ($[Fe^{III}Por]^+$) have been of current interest, because they are putative intermediates in the redox cycles or iron porphyrin complexes and heme proteins.[1] A number of spectroscopic techniques and physical measurements have been utilized to identify the electronic structures of the reduced products since 1971. In particular, two complexes, $[FeTPP]^-$ (TPP = tetraphenylporphyrin) and $[FeOEP]^-$ (OEP = octaethylporphyrin), have been examined in some detail.[2-8] For instance, electron spin resonance (ESR) signals at $g = 2.3, 1.93$ and $g = 2.24, 1.92$ were clear evidence for $[Fe^ITPP]^-$ and $[Fe^IOEP]^-$ formation.[3,9] In addition, solution magnetic susceptibility measurements for $[Fe^ITPP]^-$ and $[Fe^IOEP]^-$ gave values of 2.7 and 2.8 μ_B, respectively.[2,3] These results indicate $[FeTPP]^-$ and $[FeOEP]^-$ to be low-spin d^7 iron(I) species, consistent with Mössbauer[10] and resonance Raman[4] (RR) spectroscopic studies. In addition, $[Fe^ITPP]^-$ was revealed to have no apparent axial ligands by X-ray crystallography.[11a]

On the other hand, Reed suggested that some reduced iron porphyrin complexes ($[FePor]^-$) could involve delocalization of charge between an iron(II) porphyrin anion radical and an iron(I) porphyrin.[10] In fact, electrochemical, ESR, and RR studies of FeTPP having CN groups at the pyrrole positions ($[Fe(TPP(CN)_4)]^-$) suggested its primary structure was that of π-anion radical.[7,9] These differences in the formulation of $[FePor]^-$ indicate that the electronic structure of $[FePor]^-$ would be controlled by manipulating the lowest unoccupied molecular orbital (LUMO) of the porphyrin ring. Especially, introduction of electron-withdrawing groups at the porphyrin ring would be useful to control the electron distribution in the $[FePor]^-$ complexes.

In this paper, we report the characterization of two-electron-reduced products ($[FePor]^-$) of $Fe^{III}OEP$ and $Fe^{III}TPP$ derivatives having electron-withdrawing groups at the meso or β-pyrrole position(s) (Figure 1) on the basis of NMR, ESR, solution magnetic susceptibility, and UV–vis spectral measurements.

Experimental Section

A series of meso-substituted OEP (Figure 1a) and β-pyrrole-substituted TPP complexes (Figure 1b) were prepared by the literature methods.[12] Porphyrins were routinely characterized by UV–vis and ^{1}H-NMR spectroscopies. Meso-deuterated OEP and β-pyrrole-deuterated TPP were prepared by the usual procedures.[13] The iron(III) complexes were prepared and purified according to the procedures reported.[14] Tetrahydrofuran (THF) was refluxed with calcium hydride (CaH_2) for 3 h, distilled from fresh CaH_2, and then stirred with sodium in the presence of a small amount of benzophenone for 18 h, followed by distillation from a dehydrating agent (sodium and benzophenone). THF thus obtained was further degassed by the freeze–pump–thaw method more than five

(1) (a) McCandlish, E.; Miksztal, A. R.; Nappa, M.; Sprenger, A. Q.; Valentine, J. S.; Strong, J. D.; Spiro, T. G. *J. Am. Chem. Soc.* **1980**, *102*, 4268–4271. (b) Welborn, C. H.; Dolphin, D.; James, B. R. *J. Am. Chem. Soc.* **1981**, *103*, 2869–2871. (c) Lexa, D.; Mispelter, J.; Saveant, J. M. *J. Am. Chem. Soc.* **1981**, *103*, 6806–6812. (d) Arasasingham, R. D.; Balth, A. L.; Latos-Grazynski, L. *J. Am. Chem. Soc.* **1987**, *109*, 5846–5847. (e) Lexa, D.; Saveant, J.-M.; Su, K.-B.; Wang, D.-L. *J. Am. Chem. Soc.* **1988**, *110*, 7617–7625.
(2) Cohen, I. A.; Ostfeld, D.; Lichtenstein, B. *J. Am. Chem. Soc.* **1972**, *94*, 4522–4525.
(3) Hickman, D. L.; Shirazi, A.; Goff, H. M. *Inorg. Chem.* **1985**, *24*, 563–566.
(4) Teraoka, J.; Hashimoto, S.; Sugimoto, H.; Mori, M.; Kitagawa, T. *J. Am. Chem. Soc.* **1987**, *109*, 180–184.
(5) Lexa, D.; Momenteau, M.; Mispelter, J. *Biochim. Biophys. Acta* **1974**, *338*, 151–163.
(6) Kadish, K. M.; Larson, G.; Lexa, D.; Momenteau, M. *J. Am. Chem. Soc.* **1975**, *97*, 287–288.
(7) Kadish, K. M.; Boisselier-Cocolios, B.; Simonet, B.; Chang, D.; Ledon, H.; Cocolios, P. *Inorg. Chem.* **1985**, *24*, 2148–2156.
(8) Kadish, K. M. In *Iron Porphyrins, Part II*; Lever, A. B. P., Gray, H. B., Eds.; Addison-Wesley: Reading, MA, 1983; pp 161–249.
(9) Donohoe, R. J.; Atamian, M.; Bocian, D. F. *J. Am. Chem. Soc.* **1987**, *109*, 5593–5599.
(10) Reed, C. A. *Adv. Chem. Ser.* **1982**, *No. 201*, 333–356.
(11) (a) Mashiko, T.; Reed, C. A.; Haller, K. J.; Scheidt, W. R. *Inorg. Chem.* **1984**, *23*, 3192–3196. (b) Reed, C. A.; Mashiko, T.; Scheidt, W. R.; Spartalian, K.; Lang, G. *J. Am. Chem. Soc.* **1980**, *102*, 2302–2306.
(12) (a) Bonnett, R.; Stephenson, G. F. *J. Org. Chem.* **1965**, *30*, 2791–2798. (b) Bonnett, R.; Gale, I. A. D.; Stephenson, G. F. *J. Chem. Soc. C* **1966**, 1600–1604. (c) Johnson, A. W.; Oldfield, D. *J. Chem. Soc. C* **1966**, 794–799. (d) Callot, H. J. *Tetrahedron Lett.* **1973**, *50*, 4987–4990. (e) Callot, H. J. *Bull. Soc. Chim. Fr.* **1974**, 1492–1496. (f) Callot, H. J.; Giraudeau, A.; Gross, M. *J. Chem. Soc., Perkin Trans. 2* **1975**, 1321–1324. (g) Watanabe, E.; Nishimura, S.; Ogoshi, H.; Yoshida, Z. *Tetrahedron* **1975**, *31*, 1385–1390. (h) Smith, K. M.; Barnett, G. H.; Evans, B.; Martynenko, Z. *J. Am. Chem. Soc.* **1979**, *101*, 5953–5961. (i) Smith, K. M.; Bisset, M. F.; Tabba, H. D. *J. Chem. Soc., Perkin Trans. 1* **1982**, 581–585. (j) Gong, L.-C.; Dolphin, D. *Can. J. Chem.* **1985**, *63*, 401–405.
(13) Fajer, J.; Borg, D.; Forman, A.; Dolphin, D.; Felton, R. H. *J. Am. Chem. Soc.* **1970**, *92*, 3451–3459.
(14) Fuhrhop, J.-H.; Smith, K. M. In *Porphyrins and Metalloporphyrins*; Smith, K. M., Ed.; Elsevier: Amsterdam, 1975; p 798.

0020-1669/92/1331-3216$03.00/0

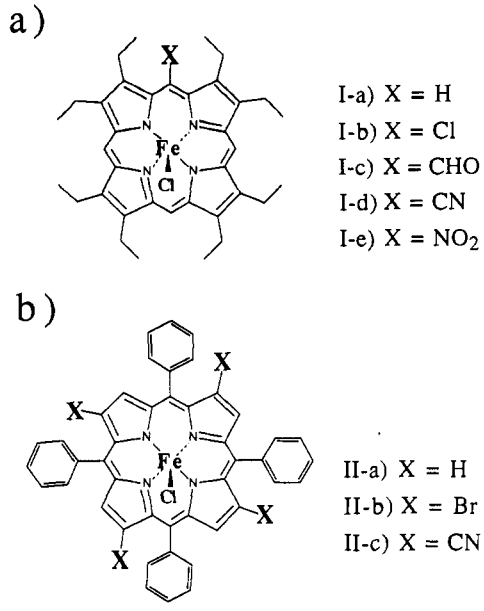

Figure 1. Iron porphyrins investigated in this work: (a) meso-substituted OEP; (b) β-pyrrole-substituted TPP.

times. The solvent (THF) was used without exposure to air in a vacuum line or in a glovebox under argon atmosphere. Reduction of [Fe^{III}OEP]Cl and [Fe^{III}TPP]Cl was carried out with sodium anthracenide as a reducing reagent in a glovebox (argon atmosphere). An alternative preparation of the reduced complexes involved Na-mirror contact in a Thunberg-type vessel in vacuo. ESR and NMR tubes and UV–vis cells were sealed with Teflon caps and wrapped with Parafilm in a glovebox. The reduced products were transferred in a vacuum line from the reaction tubes to ESR or NMR tubes, which were then sealed without exposure to air. UV–vis spectral measurements were performed on a Hitachi 330 spectrophotometer. Proton NMR spectra at 300 MHz and deuterium NMR spectra at 46.1 MHz were recorded with a Nicolet NT-300 spectrometer equipped with a 1280 computer system. Chemical shifts were referenced to Me_4Si, and downfield shifts were given a positive sign. The sample concentrations for NMR measurements were 2–5 mM. Proton NMR measurements were used to determine solution magnetic susceptibilities by the Evans method[15] employing Me_4Si/THF solutions of iron porphyrins (ca. 5 mM). Generation of the desired porphyrin species was confirmed by proton NMR spectroscopy before the measurement of splitting of two Me_4Si signals. The concentration of the Fe(III) porphyrin chloride was calculated on the basis of the known magnetic moment of 5.9 μ_B. ESR spectra were obtained on a JEOL PE-2X spectrometer modified with a JEOL ES-SCXA gun diode microwave unit by using a JES-UCD-2X liquid-nitrogen Dewar bottle. ESR microwave frequencies were counted on a Takedariken TR-5501 frequency counter equipped with a TR-5023 frequency converter.

Results

I. One-Electron-Reduction Products of Fe(III) Porphyrin Complexes. Chemical reduction of substituted ferric porphyrin complexes in THF solution was monitored by UV–visible spectroscopy. For example, Figures 2 and 3 show spectral changes of [$Fe^{III}(NO_2$-OEP)]Cl and [Fe^{III}(CHO-OEP)]Cl, respectively, upon contact with a sodium mirror. Upon reduction by the sodium-mirror contact, the absorption spectra of ferric porphyrins change to those of ferrous porphyrins with isosbestic points (Figures 2a and 3a). The absorption maxima for substituted iron porphyrin complexes employed here are summarized in Table I. Spectra of one-electron-reduced products of meso-substituted iron porphyrins were very close to that of unsubstituted Fe^{II}OEP (407, 530, and 557 nm), which was reported previously to be the five-coordinate ferrous high-spin complex (Fe^{II}OEP(THF)) by a Raman study.[4] The spectrum of [Fe($(Br)_4$-TPP)] was also similar to that of Fe^{II}TPP, while a recent X-ray crystallographic

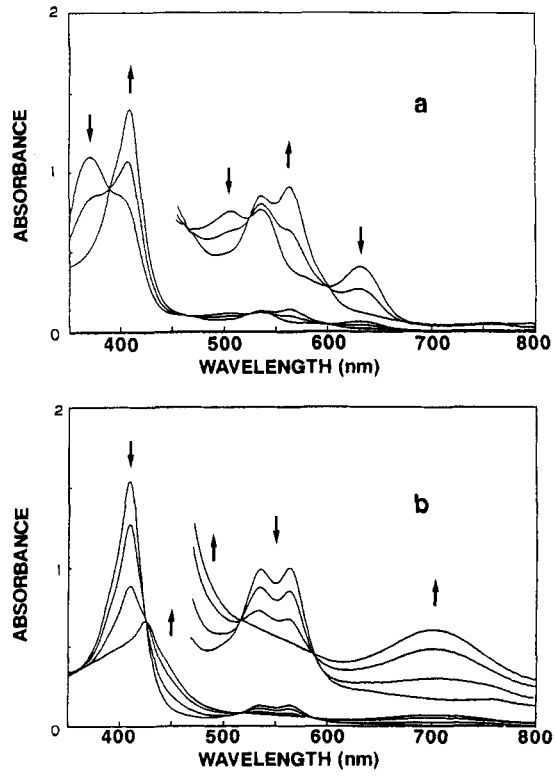

Figure 2. Absorption spectral changes upon reduction of (a) [$Fe^{III}(NO_2$-OEP)]Cl to [$Fe^{II}(NO_2$-OEP)] and (b) [$Fe^{II}(NO_2$-OEP)] to [Fe(NO_2-OEP)]$^-$ in THF by Na-mirror contact in a Thunberg-type vessel in vacuo.

analysis[11b] and an NMR spectroscopic study[3] of Fe^{II}TPP have identified its structure being a six-coordinate ferrous high-spin complex (Fe^{II}TPP$(THF)_2$). The products of the reduction of ferric complexes by sodium anthracenide in THF solution also gave the same spectra.

In order to establish the electronic structure of the one-electron-reduced form of Fe(III) porphyrin complexes, deuterium NMR spectra of meso-deuterated Fe(X-OEP) (X = H, Cl, CHO, CN, NO_2) and β-pyrrole-deuterated Fe(X_4-TPP) (X = H, Br, CN) complexes were recorded. As shown in Table II, deuterium NMR signals of Fe(X-OEP) complexes appeared in the range 3.1–22.6 ppm due to their paramagnetic shifts. While the β-pyrrole signal of the [Fe($(CN)_4$-TPP)]$^-$ complex (60.0 ppm) is downfield-shifted by 12 ppm compared to that of the unsubstituted [FeTPP]$^-$ complex, its chemical shift is still close to that of the ferrous high-spin Fe^{II}TPP butyl mercaptide complex (61 ppm).[16] The chemical shifts of one-electron-reduction products of Fe(III) porphyrin complexes obeyed the Curie law at temperatures between +25 and −80 °C. The solution magnetic moments of 4.92–5.2 μ_B for the Fe(II) porphyrin complexes employed in this study were obtained by the Evans method, indicating the complexes to be $S = 2$ systems. No EPR signals for the complexes were obtained at 77 K in THF. These results clearly indicate that the one-electron-reduced products are high-spin Fe(II) porphyrin complexes.

II. Two-Electron-Reduction Products of Fe(III) Porphyrin Complexes. A. Meso-Substituted FeOEP Complexes. The further reduction of the Fe(II) porphyrin complexes by the sodium mirror was monitored spectroscopically. The absorption spectra of the ferrous species change to those of the further one-electron-reduced products ([Fe(NO_2-OEP)]$^-$ and [Fe(CHO-OEP)]$^-$) with isosbestic points as shown in Figures 2b and 3b. Figure 3c displays spectral changes of [Fe(CHO-OEP)]$^-$ upon further contact with the sodium mirror. Inspection of Figures 3b and 3c shows that the isosbestic points in Figure 3b are different from those in Figure 3c, indicating that two-electron- and three-electron-

(15) Evans, D. F. *J. Chem. Soc.* **1959**, 2003–2005.

(16) Parmely, R. C.; Goff, H. M. *J. Inorg. Biochem.* **1980**, *12*, 269.

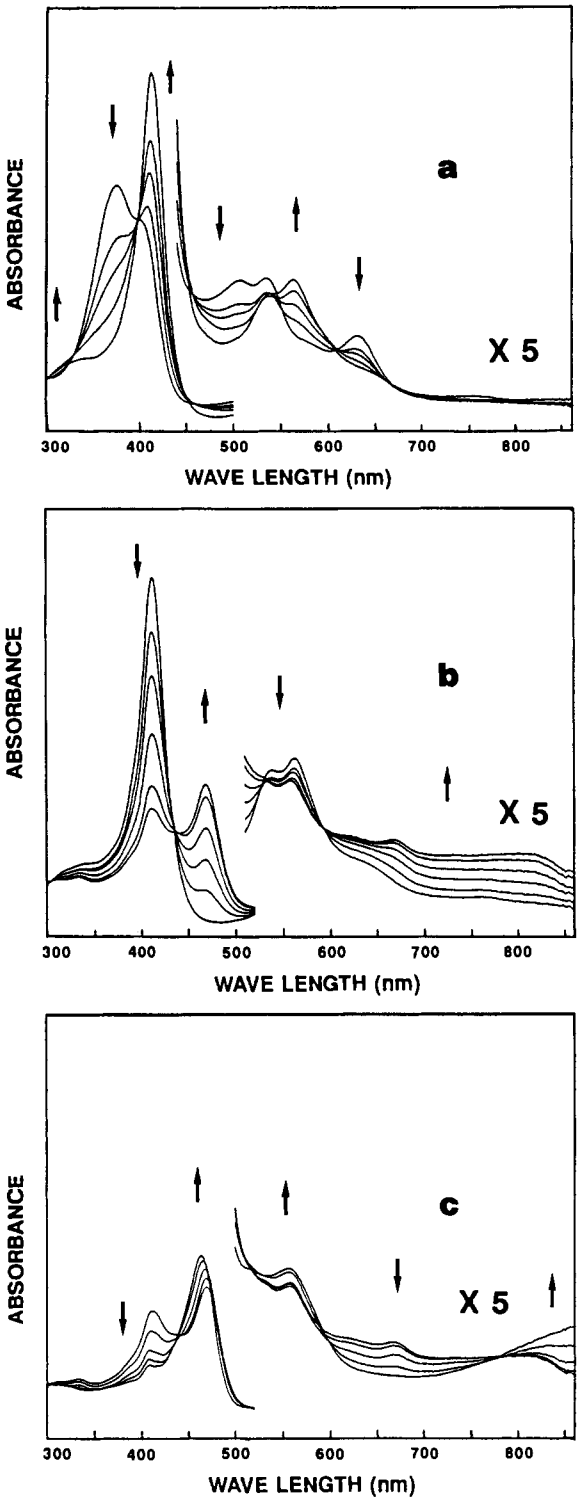

Figure 3. Absorption spectral changes upon reduction of (a) [Fe^{III}(CHO-OEP)]Cl to [Fe^{II}(CHO-OEP)], (b) [Fe^{II}(CHO-OEP)] to [Fe(CHO-OEP)]$^-$, and (c) [Fe(CHO-OEP)]$^-$ to [Fe(CHO-OEP)]$^{2-}$ in THF by Na-mirror contact in a Thunberg-type vessel in vacuo.

reduction products are formed. The absorption spectra observed when 2 equiv of sodium anthracenide as a reducing reagent was added to the ferric porphyrin solutions were the same as the spectra in Figure 3b obtained by the sodium-mirror-contact method. Accordingly, we identified the absorption spectra of two-electron-reduction product shown in Figure 3b. Similar spectral changes were observed for other meso-substituted OEP derivatives. Absorption spectra thus obtained for the [Fe(X-OEP)]$^-$ (X = H, Cl, CHO, CN, NO_2) complexes in THF are summarized in Figure 4. As shown in Figure 4, the absorption spectra of [Fe(CHO-OEP)]$^-$ and [Fe(CN-OEP)]$^-$ exhibited split Soret bands, as is frequently the case for FeTPP complexes,[10] while such split Soret bands were not observed for the other meso-substituted OEP complexes. Introduction of an electron-withdrawing group at a meso position of the OEP ring caused the Soret band to red-shift. Interestingly, the absorption spectrum of [Fe(NO_2-OEP)]$^-$ was different from those of other meso-substituted complexes in the long-wavelength region. While [Fe(NO_2-OEP)]$^-$ exhibited only a broad band at 700 nm, the other meso-substituted [Fe(X-OEP)]$^-$ complexes exhibited multiple bands in the region 500–700 nm. The spectrum observed for [Fe(NO_2-OEP)]$^-$ is similar to those reported for phlorins.[17] However, the quantitative conversion of [Fe(NO_2-OEP)]$^-$ to [Fe^{III}(NO_2-OEP)]Cl was accomplished by exposure to air and then HCl vapor. Thus, NMR spectroscopy was required for further characterization of [Fe(NO_2-OEP)]$^-$.

Figure 5 shows the deuterium NMR spectral changes of meso-deuterated Fe(NO_2-OEP) complexes upon titration of [Fe^{III}(NO_2-OEP)]Cl with a reducing reagent (sodium anthracenide). Upon one-electron reduction, signals i at −44.3 and −57.1 ppm in Figure 5a for the ferric porphyrin complexes disappeared and the new signals ii appeared at 21.2 and 3.1 ppm in Figure 5b. Upon further addition of reducing reagent, signals ii were replaced by the new signals iii in the far upfield side at −58.2 and −209.7 ppm in Figure 5d. Since 2 equiv of reducing reagent was required to obtain signals iii, signals iii are reasonably assigned to two non-equivalent meso-deuterium resonances of [Fe(NO_2-OEP)]$^-$. Other meso-substituted porphyrins exhibited quite different NMR spectral changes for their two-electron-reduction products. The NMR spectral changes for the Fe(CN-OEP) complex are exemplified in Figure 6. The NMR spectrum of the two-electron-reduction product of [Fe(CN-OEP)]Cl appears quite different from the one for [Fe(NO_2-OEP)]$^-$ and is similar to the reported spectrum of [Fe^{I}OEP]$^-$.[3] After the NMR measurements, all the solutions of the two-electron-reduction products of the meso-substituted porphyrins were exposed to air and to HCl vapor. We then recorded the NMR spectra of these solutions, which afforded the spectra of the corresponding starting ferric porphyrin complexes. This suggests that the meso-substituent groups were not reduced. The NMR results are summarized in Table II.

The deuterium NMR spectrum of [Fe(NO_2-OEP)]$^-$ exhibited unusually large paramagnetic shifts of the meso-deuterium NMR resonances (−58.2 and −210 ppm), while those of [FeOEP]$^-$, [Fe(Cl-OEP)]$^-$, [Fe(CHO-OEP)]$^-$, and [Fe(CN-OEP)]$^-$ appeared at 0–20 ppm (Table II). The unusually large paramagnetic shifts for [Fe(NO_2-OEP)]$^-$ are atypical of iron-centered paramagnetic shifts and rather appear to be similar to the shifts observed for the Fe(III) porphyrin π-cation radicals[18] and the Fe(II) *meso*-oxoporphyrin π-radical.[19] As shown in Figure 7a, the α-methylene proton resonances of [Fe(NO_2-OEP)]$^-$ are also largely shifted in the downfield region, with a pattern quite different from that for [Fe^{I}OEP]$^-$, which affords the α-methylene resonance at 3 ppm.[3] The magnetic susceptibility measurement of [Fe(NO_2-OEP)]$^-$ by the Evans method resulted in μ_{eff} = 5.7 ± 0.3 μ_B, corresponding to five spins ($S = {}^5/_2$).

The ESR spectra of the [Fe(X-OEP)]$^-$ complexes are depicted in Figures 8 and 9. It is apparent that these spectra can be classified into three types. The signals for [Fe^{I}OEP]$^-$, [Fe(Cl-OEP)]$^-$, and [Fe(CHO-OEP)]$^-$ are anisotropic and characteristic of an axially symmetric spin system. The signal of [Fe(CN-OEP)]$^-$ is rhombic (g_x = 2.03, g_y = 1.86, and g_z = 2.00) and is reminiscent of the signal observed for the five-coordinate [FePor]$^-$CO complex.[9,20] However, the ESR spectrum of

(17) Fuhrhop, J.-H. In *Porphyrins and Metalloporphyrins*; Smith, K. M., Ed.; Elsevier: Amsterdam, 1975; pp 625–666.
(18) Phillippi, M. A.; Goff, H. M. *J. Am. Chem. Soc.* **1982**, *104*, 6026–6034.
(19) (a) Sano, S.; Sano, T.; Morishima, I.; Shiro, Y.; Maeda, Y. *Proc. Natl. Acad. Sci. U.S.A.* **1986**, *83*, 531–535. (b) Morishima, I.; Fujii, H.; Shiro, Y. *J. Am. Chem. Soc.* **1986**, *108*, 3858–3860.
(20) Croisy, A.; Lexa, D.; Momenteau, M.; Saveant, J.-M. *Organometallics* **1985**, *4*, 1574–1579.

Table I. Maximum Absorbance Wavelengths (nm) for Ferric Substituted-Porphyrin Complexes and Their Reduction Products in THF

	[FePor]$^+$Cl		[FePor]		[FePor]$^-$	
compd	B band	Q bands	B band	Q bands	B bands	Q bands
[FeOEP]Cl	371	504, 530, 630	407	530, 557	372	500, 518, 569, 673
[Fe(Cl-OEP)]Cl	375	507, 537, 635	414	535, 563	409	520, 555, 623
[Fe(CHO-OEP)]Cl	375	507, 533, 632	412	533, 563	411, 469	557, 667
[Fe(CN-OEP)]Cl	377	507, 540, 635	415	556, 582	416, 434	570
[Fe(NO_2-OEP)]Cl	371	503, 535, 629	408	535, 564	427	700
[FeTPP]Cl	416	508, 572, 690	431	563, 605	390, 420	510, 580, 660
[Fe(Br_4-TPP)]Cl	432	527, 593, 674	435	530, 595	433, 454	581, 621, 675
[Fe(($CN)_4$-TPP)]Cl	443	605, 628	450	642	451, 472	622

Table II. Meso-Deuterium NMR Signals (ppm) for Iron OEP Derivatives at 23 °C

compd	[FePor]$^+$Cl	[FePor]	[FePor]$^-$
[FeOEP]Cl	−60.0 (4)	19.7 (4)	14.9 (4)
[Fe(Cl-OEP)]Cl	−57.3 (1), −60.5 (2)	24.4 (3)	15.0 (3)
[Fe(CHO-OEP)]Cl	−44.9 (1), −53.0 (2)	22.4 (1), 3.5 (2)	19.7 (1), 0.0 (2)
[Fe(CN-OEP)]Cl	−21.9 (1), −36.1 (2)	26.3 (1), 1.5 (2)	19.9 (2), 9.3 (1)
[Fe(NO_2-OEP)]Cl	−44.3 (1), −57.1 (2)	21.2 (1), 3.1 (2)	−58.2 (2), −209.7 (1)

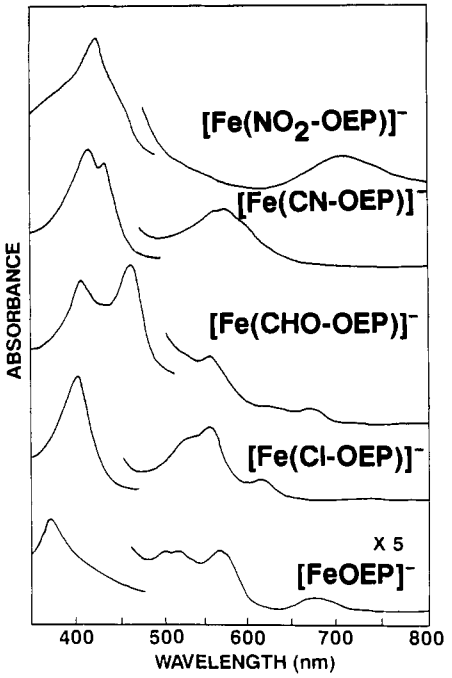

Figure 4. Absorption spectra of the meso-substituted [FeOEP]$^-$ complexes in THF.

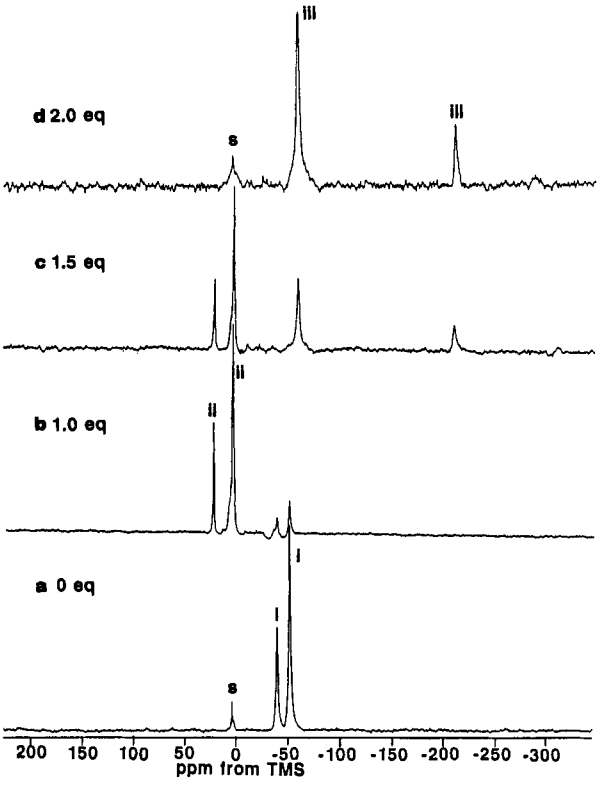

Figure 5. Deuterium NMR spectral changes for [Fe(NO_2-OEP)]Cl with addition of sodium anthracenide in THF at 23 °C. Equivalents of added sodium anthracenide: (a) 0; (b) 1.0; (c) 1.5; (d) 2.0.

[Fe(NO_2-OEP)]$^-$ is different from those of the other porphyrins. The g values (g = 5.63 and 2.00) appear to be similar to those of ferric high-spin porphyrin complexes (g = 5.91 and 1.97).

B. β-Substituted FeTPP Complexes. The reductions of Fe^{III}-TPP derivatives having substituents at the β-positions of the porphyrin ring were accomplished with sodium anthracenide in THF. The absorption maxima of [Fe(($X)_4$-TPP)]$^-$ are summarized in Table I. The characteristic split Soret bands are indicative of the formation of two-electron-reduced products, and the successive red shifts of the Soret bands parallel the order of the redox potentials for the [FePor]/[FePor]$^-$ couple.[7,9,21]

The ^{1}H NMR spectrum of [Fe(($CN)_4$-TPP)]$^-$ is shown in Figure 10. The resonance at 11.5 ppm was assigned to the β-pyrrole proton on the basis of the deuterium NMR spectrum of a β-pyrrole-deuterated compound. ^{2}H NMR chemical shifts of the β-pyrrole deuterium of [Fe(($X)_4$-TPP)]$^-$ are summarized in Table III. The β-pyrrole deuterium resonances for [Fe(($Br)_4$-TPP)]$^-$ and [Fe(($CN)_4$-TPP)]$^-$ exhibit a slight upfield bias compared with that of [FeTPP]$^-$ (29.0 ppm). The phenyl proton signals of [Fe(($Br)_4$-TPP)]$^-$ were observed in the aromatic region but were indistinguishable from those of anthracene remaining in the solution as a reducing agent. On the other hand, the phenyl proton resonances of [Fe(($CN)_4$-TPP)]$^-$ showed an alternating shift pattern: ortho and para proton signals at −0.8 and 3.4 ppm and meta proton signals at 13.7 and 14.0 ppm, respectively (Figure 10). The alternating phenyl proton shifts were also reported for TPP π-cation-radical complexes[22] and a Zn π-anion-radical complex.[3] In addition, [Fe(($CN)_4$-TPP)]$^-$ exhibited an ESR spectrum with g = 2.08 and 2.00 at 77 K in frozen THF (Figure 11, inset).

(21) (a) Kadish, K. M.; Larson, G. *Bioinorg. Chem.* **1977**, *7*, 95–105. (b) Giraudeau, A.; Callot, H. J.; Jordan, J.; Ezhar, I.; Gross, M. *J. Am. Chem. Soc.* **1979**, *101*, 3857–3862. (c) Worthington, C.; Hambright, D.; Williams, R. F. X.; Reid, J.; Burnham, C.; Shamin, A.; Turay, J.; Bell, D. M.; Kirkland, R.; Little, R. G.; Datta-Gupta, N.; Eisner, U. *J. Inorg. Biochem.* **1980**, *12*, 281–291. (d) Giraudeau, A.; Louati, A.; Gross, M.; Callot, H. J.; Hanson, L. K.; Rhodes, R. K.; Kadish, K. M. *Inorg. Chem.* **1982**, *21*, 1581–1586.

(22) Goff, H. M. In *Iron Porphyrins, Part I*; Lever, A. B. P., Gray, H. B., Eds.; Addison-Wesley: Reading, MA, 1983; pp 269–271.

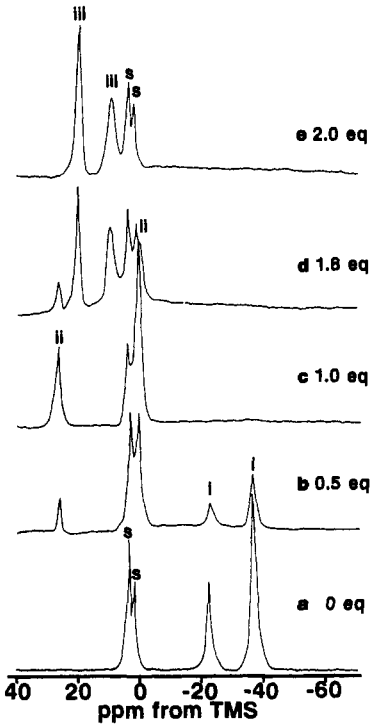

Figure 6. Deuterium NMR spectral changes for [Fe(CN-OEP)]Cl with addition of sodium anthracenide in THF at 23 °C. Equivalents of added sodium anthracenide: (a) 0; (b) 0.5; (c) 1.0; (d) 1.8; (e) 2.0.

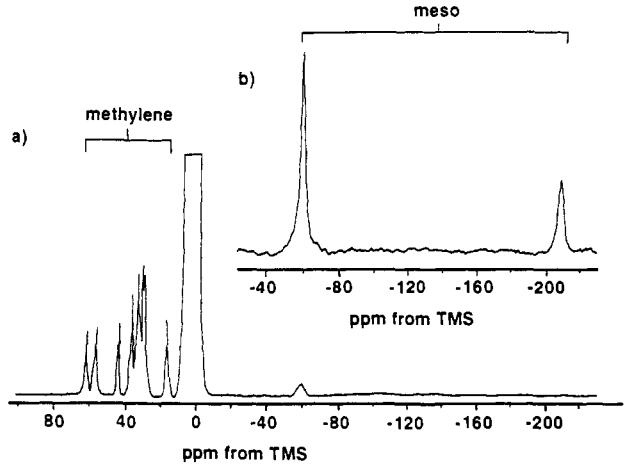

Figure 7. (a) Proton NMR spectrum and (b) deuterium NMR spectrum of meso-deuterated [Fe(NO_2-OEP)]$^-$ in THF at 23 °C.

Discussion

Characterization of Low-Valent Iron Porphyrin Complexes. NMR[23] and ESR spectra of iron porphyrin complexes are useful for distinguishing their various spin/oxidation states, and we have employed them as the principal means to determine the electronic structures of two-electron-reduced iron porphyrin complexes. For instance, the spin states of [FeTPP]$^-$ and [FeOEP]$^-$ are known to be low-spin Fe^I (d^7, $S = {}^1/_2$). Thus, the appearance of the β-pyrrole protons of [FeTPP]$^-$ and the meso protons of [FeOEP]$^-$ in a downfield region is rationalized by assuming an unpaired electron in the d_{z^2} orbital. Apparently, the chemical shift of the β-pyrrole deuterium of [Fe($(Br)_4$-TPP)]$^-$ at 22.7 ppm and the meso-deuterium signals of [Fe(Cl-OEP)]$^-$, [Fe(CHO-OEP)]$^-$, and [Fe(CN-OEP)]$^-$ (0–19.9 ppm) are quite similar to those of [FeOEP]$^-$ and [FeTPP]$^-$. These results imply that the reasonable

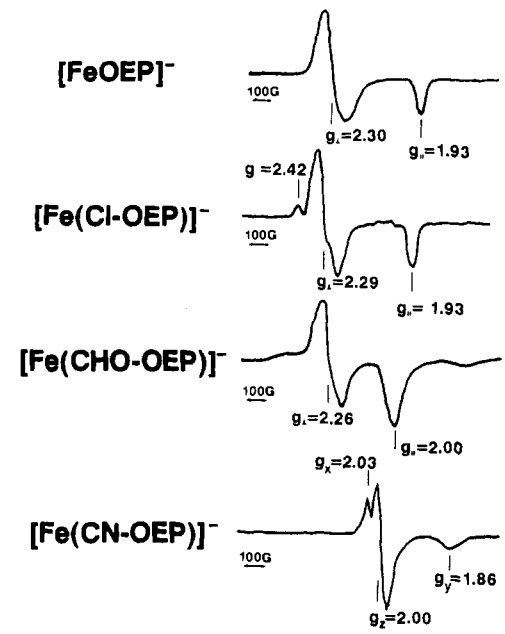

Figure 8. ESR spectra of [FeOEP]$^-$, [Fe(Cl-OEP)]$^-$, [Fe(CHO-OEP)]$^-$, and [Fe(CN-OEP)]$^-$ in THF at 77 K. The spectrum of [Fe(Cl-OEP)]$^-$ contains an impurity signal at g = 2.42.

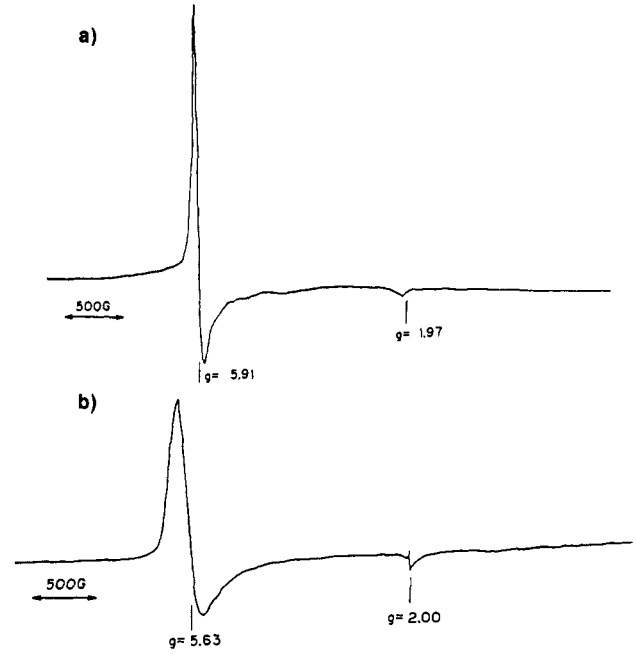

Figure 9. ESR spectra of (a) [Fe^{III}(NO_2-OEP)]Cl and (b) [Fe(NO_2-OEP)]$^-$ in frozen THF at 77 K.

spin state of [Fe(Cl-OEP)]$^-$, [Fe(CHO-OEP)]$^-$, [Fe(CN-OEP)]$^-$, and [Fe($(Br)_4$-TPP)]$^-$ is low-spin Fe^I.

The magnetic anisotropy of Fe(I) porphyrins is comparable to that of the isoelectronic Co(II) porphyrins.[24] In low-spin d^7 systems, the deviation of $g_\perp$ from 2.0 is dependent on the inverse of the $^2A_1$–^2E separation, while $g_\parallel$ remains close to 2.0. An increase in this separation decreases the magnetic anisotropy, $g_\parallel^2 - g_\perp^2$. From Figure 8, the magnetic anisotropies of [FeOEP]$^-$, [Fe(Cl-OEP)]$^-$, and [Fe(CHO-OEP)]$^-$ are calculated to be −1.57, −1.52, and −1.11, respectively. Accordingly, an electron-withdrawing substituent as a meso position of FeOEP induces greater $^2A_1$–^2E separation and eventually increases the axial ligand field. In fact, the ESR signal of [Fe(CN-OEP)]$^-$ is rhombic

(23) (a) La Mar, G. N.; Walker, F. A. In *The Porphyrins*; Dolphin, D., Ed.; Academic Press: New York, 1979; Vol. IV, pp 61–157. (b) Goff, H. M. In *Iron Porphyrins, Part I*; Lever, A. B. P., Gray, H. B., Eds.; Addison-Wesley: Reading, MA, 1983; pp 237–282.

(24) (a) La Mar, G. N.; Walker, F. A. *J. Am. Chem. Soc.* **1973**, *95*, 1790–1796. (b) Goff, H. M.; La Mar, G. N.; Reed, C. A. *J. Am. Chem. Soc.* **1977**, *99*, 3641–3646.

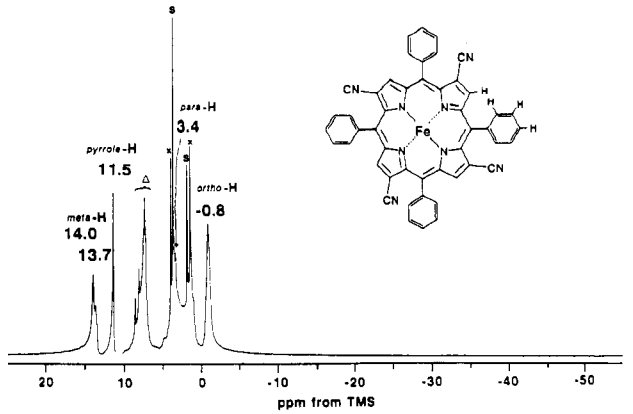

Figure 10. Proton NMR spectrum of $[Fe((CN)_4\text{-TPP})]^-$ in THF at 22 °C. Solvent (THF), impurity, and anthracene (reducing agent) peaks are labeled S, X, and Δ, respectively.

Table III. β-Pyrrole-Deuterium NMR Signals (ppm) for Iron β-Pyrrole-Substituted TPP Complexes at 23 °C

compd	$[FePor]^+Cl$	[FePor]	$[FePor]^-$
[FeTPP]Cl	80.0	48.0	29.0
$[Fe(Br_4\text{-TPP})]Cl$	75.6	49.0	22.7
$[Fe((CN)_4\text{-TPP})]Cl$	78.0	60.0	11.5

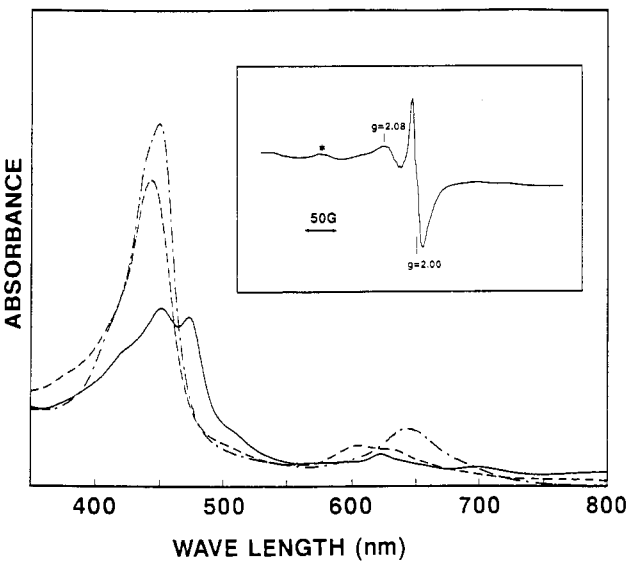

Figure 11. Absorption spectra of $[Fe^{III}((CN)_4\text{-TPP})]Cl$ (- - -), $[Fe^{II}((CN)_4\text{-TPP})]$ (- · -) and $[Fe((CN)_4\text{-TPP})]^-$ (—) in THF. Inset: ESR spectrum of $[Fe((CN)_4\text{-TPP})]^-$ in THF at 77 K. The asterisk in the ESR spectrum is an impurity signal.

(Figure 8), suggesting a stronger axial ligand field due to meso substitution of a cyano group. It further implies that the $[Fe(CN\text{-OEP})]^-$ complex has an axial ligand, which would be a solvent molecule (THF).

Introduction of a nitro group at a meso position of $[FeOEP]^-$ gave a spectrum very different from those of other meso-substituted FeOEP derivatives. As shown in Figure 2, $[Fe(NO_2\text{-OEP})]^-$ exhibits a Soret band with low intensity and a broad band at 650–750 nm which is characteristic of porphyrin π-radicals.[25] If $[Fe(NO_2\text{-OEP})]^-$ contains a π-radical spin on the porphyrin ring, unusually large paramagnetic NMR shifts of the meso proton should be observed due to contact shifts.[3] The ^2H NMR spectrum of meso-deuterated $[Fe(NO_2\text{-OEP})]^-$ shown in Figure 7 is in good agreement with these considerations.

In general, contact shifts arise from the transfer of unpaired spin density to an orbital centered on the nucleus of interest. A simple expression for the contact shift is given by

$$(\Delta H/H) = -Ag\beta S(S+1)/3\gamma_N hkT$$

where A is the contact hyperfine coupling constant reflecting the density of unpaired spin at the nucleus, while γ_N is the nuclear magnetogyric ratio. The proton coupling constant A_H is related to the attached aromatic center spin density ρ_c by the McConnell equation[26]

$$A_H = Q\rho_c/2S$$

where Q is a constant of −22.5 G. A net 230.9 ppm upfield shift (from +21.2 to −209.7 ppm) of the meso-deuterium resonance upon one-electron reduction of $[Fe^{II}(NO_2\text{-OEP})]$ is translated into 0.08 π-spin density on the meso carbon of e_g^* orbitals on the basis of McConell's relation. This value is comparable to the one obtained by a CNDO/2 MO calculation of π density (0.12) on the meso carbon of the two degenerate e_g^* orbitals ($e_{g_x}^*$ and $e_{g_y}^*$) of an iron(II) porphyrin π-anion radical. Replacement of a meso proton with a nitro group then causes these e_g^* orbitals to be at different energy levels.

The appearance of two sets of nonequivalent deuterium signals for $[Fe(NO_2\text{-OEP})]^-$ at −58.2 and −209.7 ppm with an intensity ratio of 2:1 indicates that most of unpaired spin is located in the $e_{g_x}^*$ orbital (Figure 7b). The e_g^* orbitals of $[Fe(NO_2\text{-OEP})]^-$ also allow nonequivalent amounts of spin densities on the β-pyrrole carbons. Accordingly, eight α-methylene proton resonances located in the 17–65 ppm region suggest the presence of a fifth ligand. If $[Fe(NO_2\text{-OEP})]^-$ has no axial ligand, the complex has a C_{2v} symmetry and four α-methylene proton signals must be observed. The solution magnetic susceptibility of 5.7 μ_B for $[Fe(NO_2\text{-OEP})]^-$ corresponds to $S = {}^5/_2$. If iron ($S = 2$) were strongly spin-coupled to the radical ($S = {}^1/_2$), the magnetic moment would be 3.87 μ_B (overall $S = {}^3/_2$ system). The high-spin state ($S = {}^5/_2$) of $[Fe(NO_2\text{-OEP})]^-$ appears consistent with the ESR data (g = 5.63 and 2.00) as shown in Figure 9. Accordingly, $[FeOEP(NO_2)]^-$ is formulated as a five-coordinate ferrous high-spin porphyrin π-anion radical with almost independent spins on iron and the porphyrin ring.

Recent resonance Raman,[9] ESR,[7,9] and electrochemical studies[7] on $[Fe((CN)_4\text{-TPP})]^-$ suggest its electronic structure to be that of an Fe(II) porphyrin π-anion radical. The observation of alternating NMR shifts for the phenyl protons of $[Fe((CN)_4\text{-TPP})]^-$ (Figure 10) is consistent with these results. However, if the complex were a pure porphyrin π-anion radical, more upfield paramagnetic shifts for the β-pyrrole protons would be expected. The averaged π-spin density (0.03) on the β-pyrrole carbons in the degenerate e_g^* orbitals obtained by a CNDO/2 MO calculation for a porphyrin π-anion radical predicts about −90 ppm upfield contact shift for the β-pyrrole protons. Therefore, the appearance of the β-pyrrole proton resonance at 11.5 ppm suggests that $[Fe((CN)_4\text{-TPP})]^-$ is not described as a pure porphyrin π-anion radical, but could be formulated as a resonance form between an Fe(I) porphyrin and an Fe(II) porphyrin π-anion radical.

Implication of Substituent Effects on the Electronic Structure of Low-Valent Iron Porphyrin. As discussed above, two-electron-reduced iron porphyrins can assume several electronic structures upon the introduction of electron-withdrawing substituents on the porphyrin ring. Electron-withdrawing substituents on the porphyrin ring cause two effects. One is lowering of the energy level of the porphyrin e_g orbitals. The other effect is a weakening of the interaction between the iron and the porphyrin due to the decrease in the electron density at the pyrrole nitrogens of the porphyrin ring. According to these effects, the electronic structures of two-electron-reduced iron porphyrin complexes can be roughly classified into the following four types (Figure 12).

(25) Dolphin, D.; Forman, A.; Borg, D. C.; Fajer, R. H. *Proc. Natl. Acad. Sci. U.S.A.* **1971**, *68*, 614–618.

(26) (a) Das, M. R.; Wagner, S. B.; Freed, J. *J. Chem. Phys.* **1970**, *52*, 5404–5417. (b) McConnell, H. M. *J. Chem. Phys.* **1961**, *34*, 13–16.

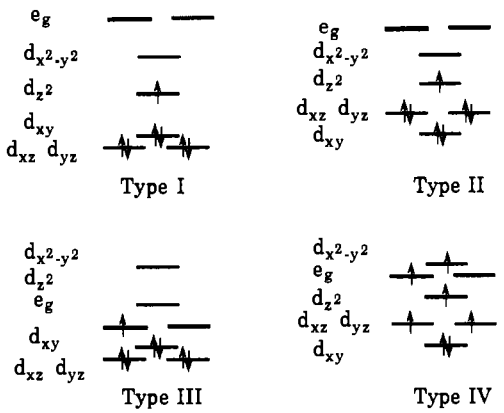

Figure 12. Schematic representation of the four types of electronic structures of two-electron-reduced iron(III) porphyrin complexes: Type I, four-coordinated iron(I) low-spin porphyrin; type II, five-coordinated iron(I) low-spin porphyrin; type III, four-coordinated iron(II) low-spin porphyrin anion radical; type IV, five-coordinated iron(II) high-spin porphyrin anion radical.

In the case of iron porphyrins having less electron-withdrawing substituents on either an OEP or a TPP ligand, such as [FeOEP]$^-$, [Fe(Cl-OEP)]$^-$, [Fe(CHO-OEP)]$^-$, [FeTPP]$^-$, and [Fe((Br)$_4$-TPP])$^-$, the energy levels of the e_g orbitals are much higher than that of the d_{z^2} orbital and there is strong ligation of the porphyrin ligand (type I). Consequently, complexes of type I are Fe(I) porphyrins bearing no axial ligand. Introduction of a CN group on the OEP ring results in a weaker ligation of the porphyrin to the central iron, forming five-coordinated Fe(I) species (type II).

Stronger electron-withdrawing substituents cause the energy levels of the e_g orbitals to be lower than that of the d_{z^2} orbital. Thus, an unpaired electron occupies the e_g orbitals instead of the d_{z^2} orbital (type III) and complexes of type III can be described as Fe(II) porphyrin anion radicals. Apparently, [Fe((CN)$_4$-TPP)]$^-$ is a case of type III. Lowering of the energy levels of the e_g orbitals of type II complexes affords five-coordinte Fe(II) porphyrin anion radicals such as [Fe(NO$_2$-OEP)]$^-$ (type IV).

Two degenerate e_g orbitals have a symmetry favoring overlap with the iron d_{xz} and d_{yz} orbitals. Accordingly, [FePor]$^-$ complexes of types III and IV could be formulated as a resonance structure between [Fe^{I}Por]$^-$ and [Fe^{II}Por$^{\bullet-}$]$^-$ due to the delocalization of the unpaired electron in the e_g and iron d_{xz} and d_{yz} orbitals, while the contribution of these structures is strongly dependent on both the overlapping of the orbitals and their energy gaps. In fact, [Fe((CN)$_4$-TPP)]$^-$, a complex of type III, shows the resonance structure due to the orbital interactions, as demonstrated by NMR spectroscopic measurements. On the other hand, the structure of [Fe(NO$_2$-OEP)]$^-$ (type IV) should be mostly described as [Fe^{II}Por$^{\bullet-}$]$^-$, since the orbital interaction in type IV complexes is less effective than that in type III complexes.

In conclusion, we have shown that there are at least four types of [FePor]$^-$ complexes by employing FeOEP and FeTPP derivatives. The electronic structure type is controlled by manipulating the orbital overlap between the e_g and d_{xz}, d_{yz} orbitals and relative energy levels of the e_g and d_{z^2} orbitals.

Acknowledgment. We are grateful to Dr. Y. Watanabe for help in preparing the manuscript.